Structure and Dynamics of Melts of Multiarm Polymer Stars

Tadeusz Pakula,*,†,‡ Dimitris Vlassopoulos,§ George Fytas,§ and Jacques Roovers||

Max-Planck-Institute for Polymer Research, Postfach 3148, 55021 Mainz, Germany, FORTH, Institute of Electronic Structure & Lasers, P.O. Box 1527, 71110 Heraklion, Crete, Greece, and National Research Council, Institute for Environmental Chemistry, Ottawa, Ontario, Canada K1A 0R6

Received July 2, 1998; Revised Manuscript Received October 19, 1998

ABSTRACT: We probe the structure−dynamics relationship in melts of star polymers with high functionality using small-angle X-ray scattering, rheology, and Monte Carlo computer simulations. These materials represent model steric soft spheres, which order in a liquidlike structure on a macromolecular scale because of the impenetrability of the cores. This is a consequence of the complex star topology, which is characterized by an inhomogeneous intrastar monomer density distribution. The signature of the structure appeares in the dynamics of these systems as a slow terminal relaxation process, in addition to the classical faster arm retraction mechanism. The slow process is attributed to the structural rearrangements of the stars within their liquidlike order and can be thought of as a reflection of their colloidal nature. We identify the dependence of this dynamic mode on the molecular parameters, i.e., star functionality and arm size.

I. Introduction

Regular star polymers, consisting typically of 3−18 arms, represent the simplest examples of branched polymers and as such they have received a great deal of attention by the scientific and technological communities, as demonstrated by the large number of relevant experimental and theoretical investigations.[1−3] The motivation for the investigation of star polymers relates to their global architecture which differs from that of linear chains. The understanding of the dynamics of simple star polymers provides the key for controlling the behavior of commercial randomly branched polymers, such as the new generation of metallocene polyethylenes.[4] On the other hand, the stars with an increased number of arms represent a limiting model case of another class of soft materials consisting of chains tethered with one end to a highly curved surface,[5] such as block copolymer micelles[6] or sterically stabilized colloidal dispersions.[7] Such multiarm stars have been successfully synthesized,[8] and their structure and dynamic behavior were recently investigated both in solution[9,10] and in the melt.[5b] The most interesting features observed in such systems, both in solution and in the melt, relate to the ordering of the stars into a liquidlike structure on the macromolecular scale and the reflection of the latter on the dynamics as an unusual, complex, slow terminal relaxation.[11] In the particular case of melts, this slow process is attributed to star rearrangements within their structure. These effects have been recently observed both experimentally and in computer-simulated systems.[5b,12] The underlying principle leading to this rich dynamic response is the topologically induced dual nature of multiarm stars, i.e., both polymeric and colloidal character; they possess two characteristic length scales, a small segmental size of 0 (nm) typical for polymers, and a large star-sphere size of 0 (μm) typical for colloids. The latter can be altered by chemically tailoring the molecular characteristics of these materials according to the desired final properties.

In this investigation, we study systematically the structure−dynamics relationship of multiarm star polymers, as well as its implications with respect to the better understanding of the physics of such topologically complex soft materials and the eventual design of new ones. In particular, we compare directly the results for different star systems and focus on the effects of the key molecular parameters, i.e., star functionality and arm size. The paper is organized as follows: section II describes the various materials used as well as the details of the experimental techniques. The results are presented in section III, whereas the main findings are discussed and compared in section IV. Finally, the main conclusions are summarized in section V.

II. Experimental Section

II.1. Materials. Samples of various model branched polymers synthesized in different laboratories have been used in this study: (i) Polyisoprene stars with arm numbers $f = 4$ and $f = 18$ and various arm lengths, N_a, were synthesized anionically and characterized in detail previously, in comparison with the behavior of linear polyisoprenes.[13,14] The main molecular parameters (the number of arms, f, the number-average molecular weight per arm, M_a, and the glass transition temperature, T_g) are listed in Table 1. (ii) Polybutadiene multiarm stars with $f = 64$ and $f = 128$ and various arm lengths $N_a > N_e$ (the latter being the entanglement molecular size) were synthesized anionically and characterized in detail.[8] The important molecular characteristics are given in Table 2. (iii) A polystyrene macromonomer with 10 arms, consisting of 12 monomeric backbone units, each with a polystyrenic side chain of size $M_a = 10\,000$, was synthesized with the addition-first method.[15]

II.2. Small-Angle X-ray Scattering (SAXS). SAXS experiments were performed only for the multiarm polybutadiene stars at room temperature under vacuum. A Kratky-Compact camera (Anton Paar KG) equipped with a one-dimensional position sensitive detector was used. Scattered intensities were collected by means of a multichannel analyzer and were subsequently corrected for absorption, background scattering, and slit length smearing. Primary beam intensities (Ni-filtered Cu Kα radiation) were determined in absolute units using a moving slit method.

† Max-Planck-Institute for Polymer Research
‡ Also at the Institute of Polymers of the Technical University of Lodz, Poland.
§ FORTH.
|| Institute for Environmental Chemistry.

10.1021/ma981043r CCC: $15.00
Published on Web 12/01/1998

Table 1. Characteristics of Polyisoprene Stars

sample	f	M_a	T_g, °C
PI4-15	4	15 000	−59.6
PI4-30	4	30 000	−60.8
PI4-95	4	95 000	−59.5
PI18-03	18	3 500	−59.9
PI18-12	18	12 100	−60.1
PI18-44	18	44 100	−60.5

Table 2. Characteristics of Polybutadiene Multiarm Stars

sample	f	M_a	T_g, °C
PB-155	linear	155 000	−96
PB4-11	4	11 250	−96
PB64-07	62	6 330	−92
PB64-30	56	23 900	−92
PB128-07	124	6 800	−92
PB128-14	125	13 000	−92
PB128-28	114	26 100	−92
PB128-56	127	47 000	−92

II.3. Mechanical Spectroscopy. Dynamic mechanical measurements were performed by means of the Rheometric Scientific RMS-800 and ARES-2KFRTN1 mechanical spectrometers. Shear deformation was applied under conditions of controlled deformation amplitude, always remaining in the range of the linear viscoelastic response of studied samples. Frequency dependencies of the storage (G') and loss (G'') shear moduli were measured at various temperatures, ranging from the glass transition to 150 °C. For measurements at lower temperatures, where the storage modulus was higher then 10^4 Pa, a geometry of parallel plates with diameters of 6 mm was used, whereas at higher temperatures the measurements were performed with the cone-plate geometry of 25 mm diameter. In the case of the plate−plate geometry, the gap between plates (sample thickness) was about 1 mm. Experiments were performed under dry nitrogen atmosphere.

Frequency dependencies of G' and G'' measured within the frequency range 0.1−100 rad/s at various temperatures were used to construct master curves representing the broad range frequency dependencies of these quantities. Only shifts along the frequency scale were performed. This procedure provided the temperature dependence of the shift factors (log a_T vs T). The relaxation times determining the Newtonian flow range at low frequencies were obtained from the crossover point of the extrapolated straight lines that define the characteristic behavior of $G' \sim \omega^2$ and $G'' \sim \omega$ in this regime. Relaxation times corresponding to the transition to the glassy range at high frequencies were determined as $\tau(T_{ref}) = 2\pi/\varpi_c$, where ϖ_c is the frequency at which the G' and G'' dependencies cross each other at the reference temperature.[16] Both procedures are illustrated in Figure 1 for a linear entangled polyisoprene melt. Relaxation times at other temperatures are then given by $\tau(T) = \tau(T_{ref}) + \log a_r$.[16]

II.4. Simulation Conditions. Model systems representing melts of polymer stars with various numbers of arms and various arm lengths were simulated using the cooperative motion algorithm (CMA).[12] This simulation method is suitable for dense systems of well-defined topologically complex molecular objects. Their applications to dense systems of comb polymers and star polymers have been described in detail elsewhere.[14] In this type of simulation, ensembles of beads on a lattice are connected by nonbreakable bonds to objects representing macromolecules of a specific topology. A face-centered cubic lattice is used with usually all lattice sites occupied in order to represent dense systems such as polymer melts. The systems are considered under the excluded volume condition, which means that each lattice site can only be occupied by a single molecular element (bead). In such systems strictly cooperative dynamics is used consisting of rearrangements satisfying local continuity of the simulated system (no empty lattice sites are generated). This is realized by local motions consisting of displacements of a certain number of molecular elements along closed loops so that each element replaces one of its neighbors and so that the sum of displacements of elements taking part in the rearrangement is zero (continuity condition). During such rearrangements the models of macromolecules undergo conformational transformations preserving, however, their identities given by the number and sequences of elements in the polymer and by the topology of bond skeletons joining them into a molecular object.

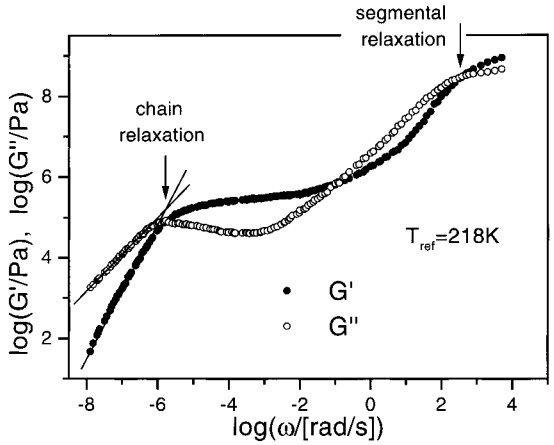

Figure 1. Typical example of G' and G'' dependencies (master curves) on frequency for a melt of linear polyisoprene chains with M_w=130 000. Arrows indicate two well-distinguished relaxation processes corresponding to segmental and chain relaxations at high and low frequencies, respectively. Solid lines with slopes 2 and 1 represent typical G' and G'' dependencies, respectively, in the Newtonian flow range of the melt.

To represent melts of the starlike molecules, model systems with polymers consisting of linear flexible chains connected to central highly branched structures have been generated. Systems with star polymers of various arm length (N_a) ranging between 10 and 80 and various numbers of arms (f) ranging between 2 and 64 have been considered. Model systems consisting of about 30 000 of beads have been simulated. The number of stars in the system was dependent on both parameters f and N_a. Periodic boundary conditions have been used and the simulation is considered as athermal. The systems have been simulated at densities of about 0.95. Nonoccupied lattice sites have been regarded as vacancies. Initially ordered systems of chains have been "molten" and carefully equilibrated in the athermal state. Vanishing orientation correlations of the initial state and displacements of chains larger than model sizes have been used as a criterion of equilibrium. For so-equilibrated states, various static and dynamic properties have been determined. A more detailed and comprehensive description of both the simulation method and the results concerning melts of stars is presented elsewhere.[12]

III. Results

III.1. Structure. All samples studied in this work were optically transparent, as it is characteristic for amorphous homopolymers. The specific molecular constitution of polybutadiene multiarm stars having the carbosilane dendrimeric centers yielded an electron density contrast between the centers and the polybutadiene arms. For these samples, SAXS experiments have been performed in order to detect the position correlation between star centers. X-ray small angle scattering intensity distributions recorded as a function of the scattering wave vector, $s = q/2\pi$, for polybutadiene samples with arm number $f = 128$ and various arm lengths are shown in Figure 2. In the two samples, PB128-07 and PB128-14, with smaller arm sizes, intense, well-resolved peaks are observed with maximum intensities at $s = 0.094$ nm^{-1} and $s = 0.074$ nm^{-1}, respectively. The first scattering peak shifts to smaller s values with increasing arm length and loses intensity,

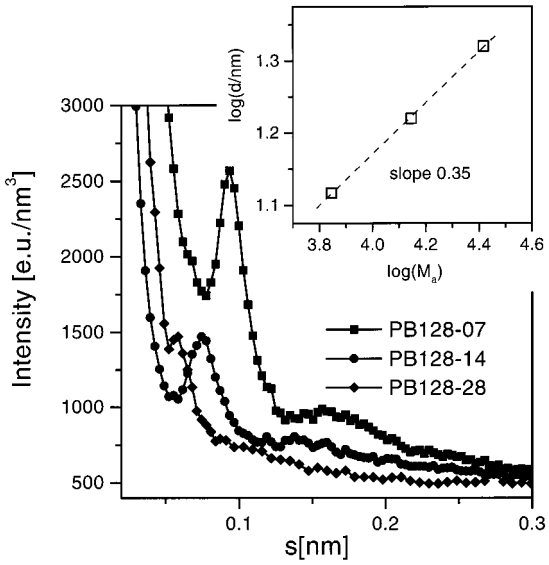

Figure 2. Small-angle X-ray scattering intensity distributions recorded for polymer melts of polybutadiene multiarm stars with the number of arms $f = 128$ and various arm lengths. The insert shows the arm molecular weight (M_a) dependence of the separation of the ordered star centers (d) determined from the position of the scattered intensity maxima. The dashed line in the insert represents a linear fit to the data indicating the dependence $d \sim M_a^{0.35}$.

so the sample PB128-28 exhibits practically only a weak hump at small angles, close to the resolution limit of the apparatus, whereas for the sample PB128-56, no maximum has been detected. The shift of the peak relates to the increase of star distances with increasing arm length, and the weakening of their intensity can be caused by two effects, i.e., a decrease of concentration of star centers per unit volume and a decrease of their center-to-center distance correlation.

For the sample PB128-07, besides the first intense peak, much less intense higher order maxima can be observed at higher s values, being approximately in positions $\sqrt{3}$ and $\sqrt{7}$ with respect to the position of the first sharp peak. This indicates a structure of an ordered liquid state, as observed, for example, in liquid mercury.[17] The positions of the higher order maxima can suggest an fcc lattice, but their low intensities indicate that this type of order is only weakly developed. To determine the distances between nearest neighboring star centers, we have used the formula $d = a/s_{max}$, where $a = 1.22$ for a fcc lattice or $a \approx 1.23$ for a structure controlled only by a two-body correlation.[17] Using the latter value of a, we obtain $d = 13.1$ nm, $d = 16.6$ nm, and $d = 20.9$ nm for PB128-07, PB128-14, and PB128-28 samples, respectively. In a dense system such as a polymer melt, the same values can be regarded as an approximation of star sizes and should satisfy the relationship $d \sim M^{1/3}$, which they do with a satisfactory accuracy, as illustrated in the inset of Figure 2.

Computer simulation of model systems representing melts of star macromolecules also provided additional strong evidence of ordering when the functionality increases. The structure of simulated systems has been characterized by the pair correlation functions of the star centers of mass ($g_{cm}(r)$), by mass distribution of beads around the center of mass of stars ($\phi_c(r)$), and by the mean square radius of gyration of stars ($\langle s_s^2 \rangle$).[5b,12] Figure 3 shows examples of the pair correlation functions of center of mass for systems with constant arm

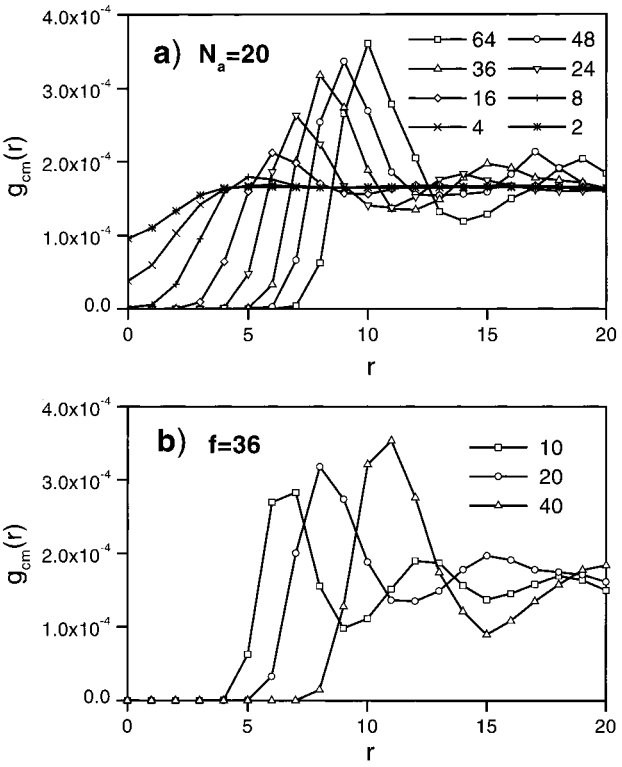

Figure 3. Pair correlation functions of the star centers of mass in computer-simulated melts of stars: (a) with constant arm length $N_a = 20$ and variable functionality f and (b) with constant f and varying arm length.

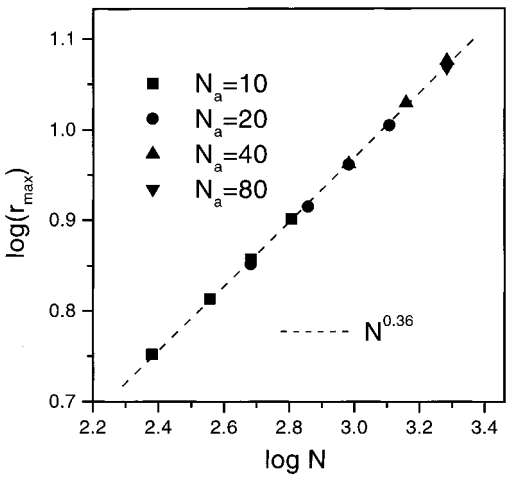

Figure 4. Positions of the main maxima in the pair correlation functions of Figure 3 as a function of the total molecular size of simulated multiarm stars ($N = fN_a$). Results for various arm numbers and various arm lengths are shown. The dashed line represents a linear fit to the data with slope 0.36.

length $N_a = 20$ but varying functionality f (Figure 3a), as well as for systems with constant f (=48) and varying N_a (Figure 3b). For stars with a small number of arms only the correlation holes are observed, whereas the stars with number of arms $f > 24$ exclude each other in space and their centers of mass assume well-defined relative positions indicated by distinct maxima in $g_{cm}(r)$. The maxima in the pair correlation functions indicate a strong position correlation between stars having larger functionality. The positions of the maxima correlate with the sizes of the stars, as seen in Figure 4, where they are presented as a function of the total number of elements within stars ($N = fN_a$). The dashed

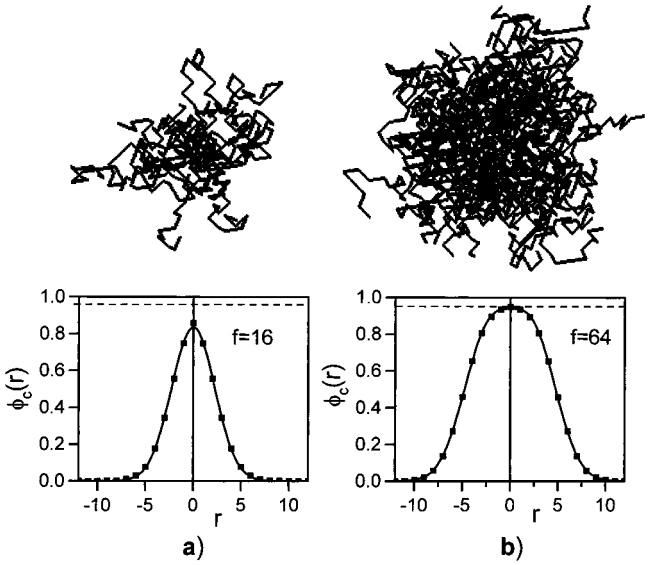

Figure 5. Distributions of density around the center of mass within stars with various numbers of arms (a) $f = 16$ and (b) $f = 64$. Model structures of corresponding stars taken from equilibrated melts are also illustrated. The horizontal dashed lines represent nominal densities of melts.

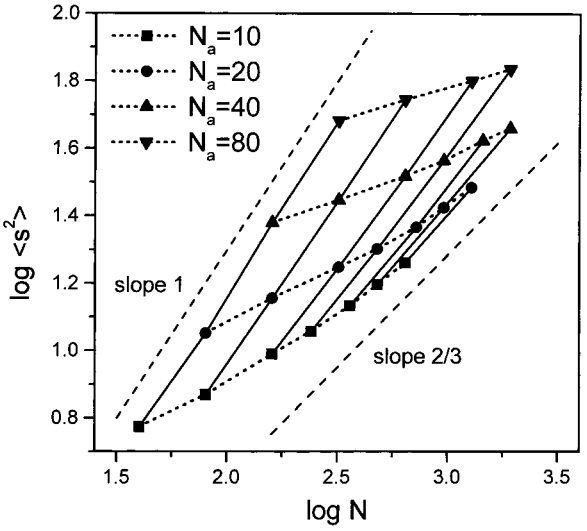

Figure 6. Mean square radius of gyration of stars in simulated melts as a function of their total mass ($N = fN_a$). Dashed lines with slopes 1 and $^2/_3$ represent scaling laws corresponding to changes of dimensions of Gaussian linear chains and densely packed compact spheres, respectively.

line represents a linear fit to the data points and indicates that both dependencies $d \sim f^{1/3}$ and $d \sim N_a^{1/3}$ (where d is the most probable separation of star centers) are satisfied with reasonable accuracy. The dependence on N_a is in good agreement with the experimental result of Figure 2.

Figure 5 shows two examples of simulated star macromolecules with the number of arms $f = 16$ and $f = 64$ and arm length $N_a = 20$, along with the corresponding distributions of their monomer density, averaged over many states in equilibrium. The maximum density within stars with $f \leq 16$ is considerably smaller than the average density of the system (indicated by the horizontal dashed line), while for stars with $f = 64$ the density at the center of the star reaches the nominal density of the system. This suggests that the stars with smaller f interpenetrate each other, but when $f > 24$, the centers of stars become impenetrable to elements of other stars.[5b,12] A detailed analysis of the intrastar monomer density distributions has shown that for stars with functionality $f > 24$ a core region can be distinguished which is almost impenetrable by elements of neighboring stars.[12] This effect indicates a strong excluded volume interaction and causes the observed position correlation of stars with respect to the neighbors, as indicated by the pair correlation functions shown in Figure 3. The drop of $g_{cm}(r)$ to zero at small r values for multiarm stars indicates a range of excluded distances between the centers of mass of nearest neighbors.

The changes of intrastar packing densities with the functionality of stars can also be observed in the dependencies of star spatial sizes, characterized by the mean square radius of gyration, $\langle s^2 \rangle$, on the number of elements, N, constituting the stars. Such results for the simulated systems are presented in Figure 6. They indicate a weak dependence of star sizes on the number of arms (dashed lines), which suggests that the main changes associated with an increase of star mass at constant arm length must relate to changes in the packing of chain elements within stars. The results in Figure 6 also show that the size of stars with a small functionality is controlled by the arm size having nearly Gausssian conformation, which scale as N (polymerlike behavior), whereas the size of stars with large f and short arms tends to approach the size of compact spheres consisting of N elements, which should scale as $N^{2/3}$. The two limiting dependencies are shown in the figure by dashed lines having the corresponding slopes. These results are in agreement with the scaling predictions of Daoud and Cotton[18a] for the size R ($\sim f^{(1-\nu)/2} N_a^{\nu}$, ν being the Flory exponent) of a spherical polymer brush in a good solvent, which have been confirmed experimentally for block copolymer micelles.[18b]

It should be noted that the parameter range in which the dependence $\langle s^2 \rangle \sim M^{2/3}$ for the star polymers in the melt is predicted has not yet been reached for real systems. This could cause differences observed in the dynamics between simulated and real systems, as described later in this paper.

III.2. Dynamics. Information about the dynamics in polymer melts of stars has been obtained from dynamic mechanical measurements. We start with the presentation of results for stars with a low number of arms in order to demonstrate later differences between their behavior and that of melts of multiarm stars. Figure 7 shows frequency dependencies (master curves) of G' and G'' for polyisoprene melts of stars with various arm lengths and two different arm numbers $f = 4$ and $f = 18$. In all cases, two well-distinguishable relaxation processes are observed: the high-frequency relaxation attributed to the segmental motion (the α process) and the low-frequency relaxation attributed to the orientational relaxation of linear chains or star arms[5b,14] ("terminal" process). Whereas the segmental relaxation is not affected by changes of the two parameters of the stars, the number of arms and arm length, the low-frequency relaxation is strongly influenced by the arm length.[3,19] The relaxation times determined by the crossover points of G' and G'', which is observed at the transition to the Newtonian flow range at low frequencies, are shown in Figure 8 as a function of the arm molecular weight. These terminal relaxation times are normalized by the relaxation times of the segmental motion, which makes the results independent of tem-

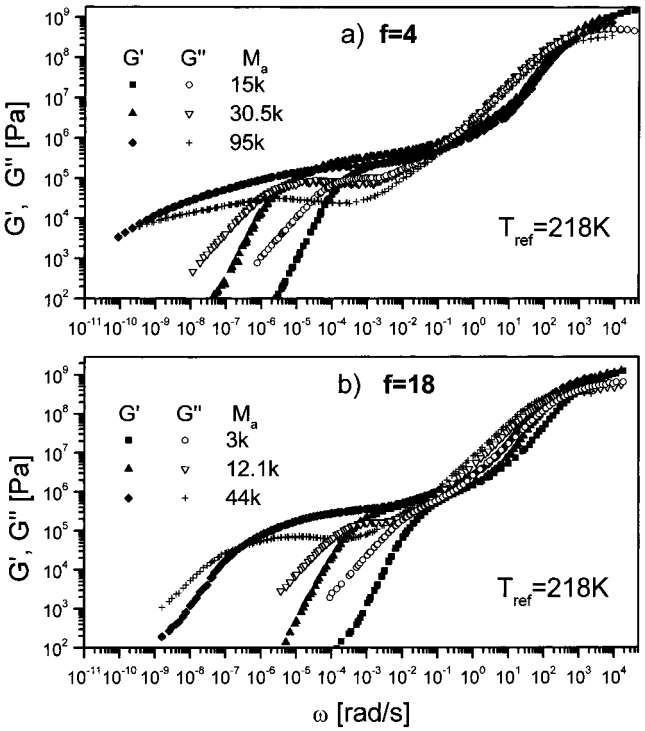

Figure 7. Frequency dependencies of the shear storage, G', and loss, G'', moduli (master curves) for melts of polyisoprene stars with various arm lengths and two different functionalities: (a) $f = 4$ and (b) $f = 18$.

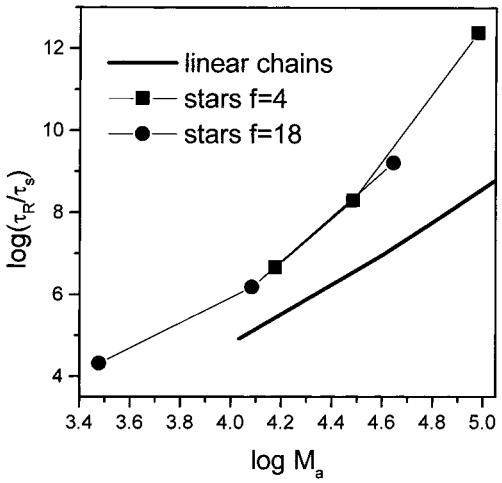

Figure 8. Arm molecular weight dependence of the terminal relaxation times, τ_R, normalized by the segmental relaxation times, τ_s, for polyisprene stars with various arm lengths and two different functionalities: (a) $f = 4$ and (b) $f = 18$. The thick solid line represents the chain length dependence of the normalized terminal relaxation times for melts of linear polyisoprene chains.[14]

perature and free of effects related to the chain length dependence of the segmental motion usually observed for short chains. The results show that these normalized relaxation times are strongly dependent on arm length of stars, but it is difficult to resolve any dependence on the arm number. The data available, however, suggest that τ_R times are essentially independent of f, in agreement with theoretical predictions[19] and previous experiments with low-functionality stars.[20] The dependence of the relaxation times on arm length is also much stronger than that observed for linear chains within the corresponding chain length range (solid line in Figure 8).[14]

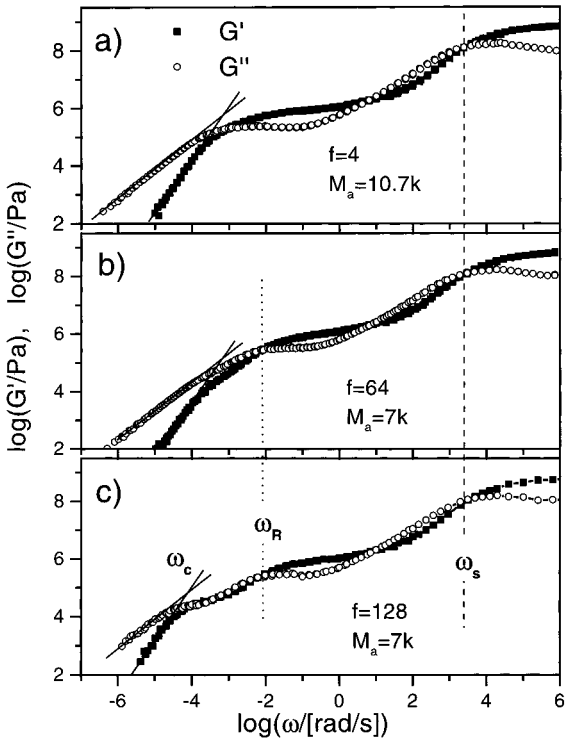

Figure 9. Examples of frequency dependencies of G' and G'' for melts of polybutadiene stars with different functionalities: (a) $f = 4$, (b) $f = 64$, and (c) $f = 128$. Vertical dashed and dotted lines mark frequencies ω_s and ω_R, corresponding to the segmental and star arm relaxations, respectively. Solid lines approximating G' and G'' dependencies at low frequencies have the same meaning as in Figure 1.

Melts of stars having a considerably higher numbers of arms than those described above show qualitatively different behavior when studied by means of the mechanical spectroscopy. Examples of the frequency dependencies of G' and G'' for such samples are shown in Figure 9 for polybutadiene melts. In the case of four-arm stars, the same behavior as described above is observed, whereas for stars with larger number of arms, $f = 64$ and f=128, the transition between the rubbery plateau and the terminal flow cannot be considered as a single relaxation process. The crossover of G' and G'' at low frequencies for the latter samples is considerably shifted with respect to the crossover of the extrapolated G' and G'' dependencies in the terminal flow range. This suggests more than one relaxation process in this frequency range. This effect is more clearly seen for stars with $f = 128$ (Figure 9c), where two crossing points of G' and G'' are observed, indicating two relaxation processes separated by a short G' plateau in the frequency range 10^{-4}–10^{-3} rad/s. This kind of behavior at low frequencies has been observed for all polybutadiene samples with number of arms $f = 64$ and $f = 128$, as is presented in Figure 10. Consequently, these samples are characterized by three relaxation times, corresponding to frequencies marked in Figure 9c as ω_c, ω_R, and ω_s. Frequencies ω_s and ω_R are defined by the crossover points of G' and G'', whereas, ω_c is assigned to the crossover point of the extrapolated low-frequency G' and G'' dependencies.

The high-frequency relaxation ω_s (indicated in Figure 9 by a vertical dashed line) is the segmental relaxation. This relaxation is not influenced markedly by the change of the arm number or arm length, and its position on the frequency scale is identical with the

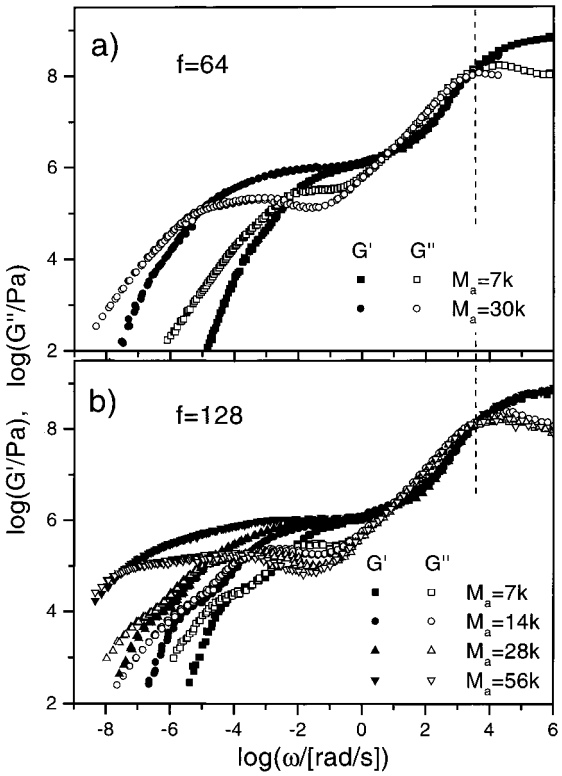

Figure 10. Frequency dependencies of G' and G'' for melts of multiarm polybutadiene stars with various arm lengths and two different functionalities: (a) $f = 64$ and (b) $f = 128$.

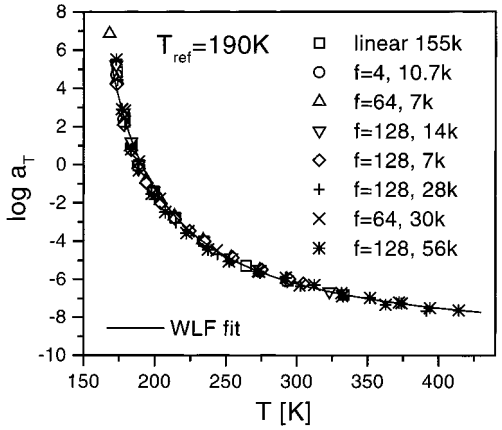

Figure 11. Temperature dependence of the shift factors used by the construction of master curves for various polybutadiene samples with different functionalities f and molecular weights per arm, M_a.

segmental relaxation observed for long ($M_w > 10^4$) polybutadiene linear chains. For all polybutadiene samples studied here, almost the same thermorheological behavior has been observed as demonstrated in Figure 11 by means of temperature dependencies of the shift factors determined by the master curve construction. Small differences observed between different samples are attributed to the inaccuracy of the shifting procedure. The WLF relation

$[\log a_T = -c_1(T - T_{ref})/(c_2 + T - T_{ref})]$ has been fitted to all data presented in Figure 11, giving $c_1 = 11.8$ and $c_2 = 50$ at $T_{ref} = 179$ K.

A comparison of the low-frequency parts of Figures 9b and 9c indicates that the frequency ω_R is not influenced remarkably by the arm number but is strongly dependent on the arm length, as can be seen

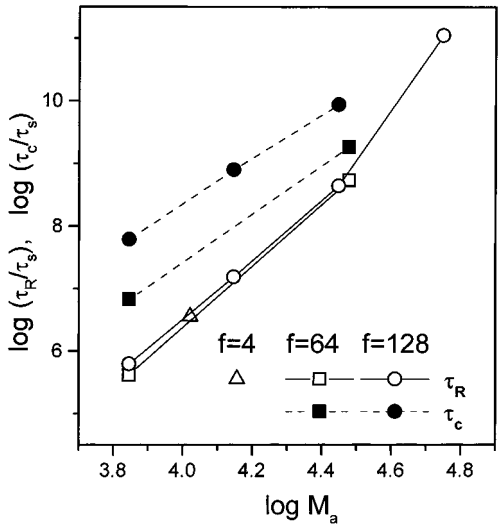

Figure 12. Arm molecular weight dependence of the relaxation times, τ_R and τ_c, both normalized by the segmental relaxation times, τ_s, for polybutadiene stars with various functionalities.

in Figure 12. Therefore, this relaxation in the multiarm stars is assigned to star arm relaxation.[19,20] A striking effect of the increase of arm number is, however, observed in the terminal relaxation region at ω_c. It is seen (Figures 9b,c and 10) that the change in the number of arms influences more strongly the relaxation at ω_c than the high-frequency component of the terminal relaxation (at ω_R). The slow relaxation is absent in all stars with low functionality (Figures 7 and 9a) and, for the multiarm stars, separates more and more distinctly from the arm relaxation with an increasing number of arms (compare parts a and b of Figure 10). This relaxation is attributed to some cooperative rearrangements of stars within the structured melts and will be discussed in detail later. The relaxation times of the two low-frequency processes, τ_c and τ_R, determined for all systems and normalized by respective segmental relaxation times, τ_s, are shown in Figure 12 as a function of the molecular weight of the arm. The results indicate that the times τ_R constitute an arm length dependence, which is common for all stars independent of the number of arms. On the other hand, the arm length dependence of the slower relaxation, τ_c, is slightly weaker and considerably influenced by the number of arms. For the sample with the longest arms, PB128-56, the observed low-frequency relaxation has been assigned as the arm relaxation; however, the dependencies in Figure 12 could suggest also the possibility of another assignment. Unfortunately, for this sample the limited thermal stability of the polymer does not allow extension of the master curve to lower frequencies than those shown in Figure 11. For that same reason we did not measure the biggest star available (128-80).

The dynamics in simulated systems representing multiarm star melts has been observed by monitoring various time correlation functions. Figure 13 shows exemplary results (more details are published elsewhere[12]). Local dynamics in model systems is characterized by the segment position autocorrelation function, $\rho_s(t)$; relaxation of star arms is described by the autocorrelation function of the center-to-end vectors of arms, $\rho_R(t)$; and the motion of whole stars is observed as the autocorrelation of positions of all star elements, $\rho_c(t)$, as well as by the mean square displacements of the

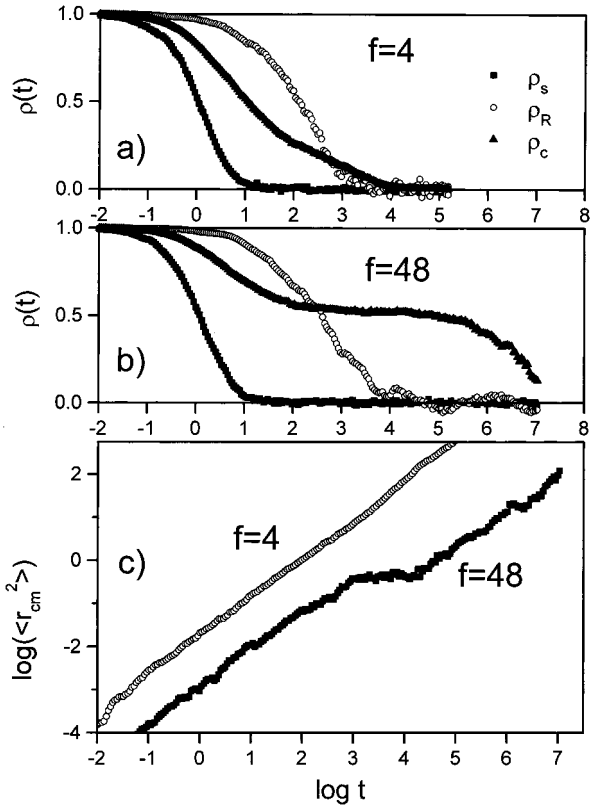

Figure 13. A comparison of various time correlation functions for simulated melts of stars with arm length $N_a = 20$ for two numbers of arms: (a) $f = 4$ and (b) $f = 48$. The correlation functions ρ_s, ρ_R, and ρ_c describe relaxation of segments, star arms, and whole stars, respectively. In panel c, mean square displacements of star centers of mass for systems with $f = 4$ and $f = 48$ are compared.

centers of mass of the star. Figure 13a−c shows examples of these correlation functions for systems differing in the arm number within the stars having a constant arm length ($N_a = 20$). In all systems independent of the number of arms, the segmental relaxation is the same. Results in Figure 13a describe the behavior of stars with a small number of arms, $f = 4$. In this case, the dynamics is mainly controlled (the slowest process) by the relaxation of the center-to-end vector, which is mainly influenced by the orientational relaxation of the arms. The situation changes considerably when the number of arms in the star becomes high ($f > 24$). Whereas, the arm relaxation changes only slightly with an increase in the arm number, the position correlation of stars becomes long-living, with the slow component of this relaxation considerably exceeding the relaxation time of the arms. The faster component of the position correlation of the star can be attributed to a relaxation of star form (as deformable objects), but for stars with a large number of arms which almost completely fill the space around the mass center, a complete relaxation must be related to translational motion of the whole star by a distance comparable with the star's size. Therefore, the slow component of the position correlation has to be attributed to a translational motion of stars beyond the originally occupied space; in an ordered system this can only take place cooperatively with some neighbors. This type of relaxation exceeds the size scale of a single star and becomes, therefore, the slowest in the system.[21]

Figure 14 shows dependencies of relaxation times determined from the above correlation functions on the number of arms. The segmental relaxation rate (τ_s) is

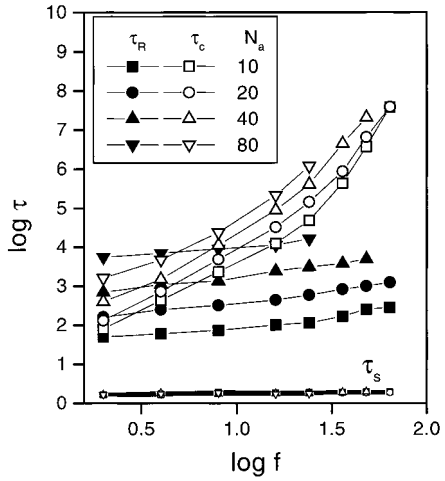

Figure 14. Dependencies of various relaxation times on arm number, f, determined for simulated systems with stars of various arm lengths, N_a. The relaxation times τ_s, τ_R, and τ_c correspond to relaxation of segments, relaxation of star arms, and to position relaxation of stars (slow structural relaxation), respectively.

expectedly independent of the arm number, in agreement with the experiments. A weak dependence on the number of arms is also observed for the arm relaxation times (τ_R). Contrary to that, the relaxation times τ_c characterizing star displacements (structural relaxation) increase very fast for the large number of arms, and this relaxation process becomes the slowest one for multiarm stars (high f). On the other hand, comparing the dependencies for various arm lengths, it is possible to notice that the arm relaxation times are more strongly influenced by the length of arms, compared to the position relaxation times, which is in agreement with the experimental results as discussed below (see also Figure 16). The range of arm lengths for simulated stars corresponds to lengths of linear chains for which a dynamics characteristic for nonentagled melts has been observed.[14] The entanglement length for such linear chain melts can be estimated as $N_e \approx 400$. Unfortunately, limits on the sizes of model systems and on computation rates do not allow examination of the entanglement regime for simulated melts of stars.

The mean squared displacements of centers of mass of stars shown in Figure 13c indicate also a distinct qualitative difference in the nature of diffusion between stars with a small and large number of arms. The stars with low functionality ($f = 4$) can smoothly displace in the whole observed displacement range by nearly random diffusive motion ($\langle r_{cm}^2 \rangle \sim t$). Contrary to that behavior, for stars with a large number of arms ($f = 48$), a distinct plateau in the time dependence of the mean square displacements is observed, indicating a freedom of star motion at short distances (in "cage" diffusion) but considerable hindrance for large excursions, which leads to a drastic slowing down of the diffusion over distances exceeding star sizes. This is in agreement with self-diffusion measurements (with pulsed field gradient NMR) on concentrated solutions of multiarm stars.[21] The bimodal translational relaxation of stars can also be noticed qualitatively by observing the form of trajectories of the centers of mass of multiarm stars in simulated melts. A typical example of such trajectory is shown in Figure 15. Such trajectory indicates that the displacement of the star is not uniform in time. The trajectory is composed of fragments in

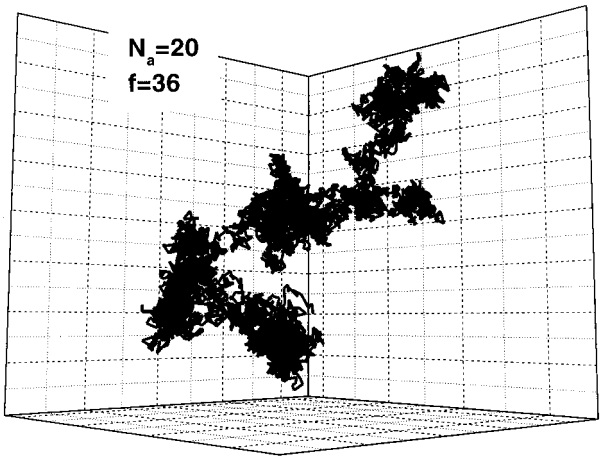

Figure 15. A typical star center of mass trajectory recorded for a multiarm star in the simulated melt. The trajectory consists of blobs related to a longer residence of the star at some well-distinguished places which are regularly distributed along the trajectory and are connected by thinner trajectory fragments related to faster displacements between the localized states.

which the motion consists of limited excursions from some quasilocalized positions (black blobs) which are connected by other fragments, indicating occasional faster displacements between these quasistable states. In this way, it has been observed qualitatively that both the amplitude of the excursions and the time of residence of a star in the localized state are strongly dependent on the arm number and arm length. The strongest localization (i.e. long residence time and small amplitude of excursions) has been observed for stars with a large number ($f = 64$) of short arms ($N_a = 10$).

IV. Discussion

We have presented results obtained experimentally for real star polymer melts and by means of computer simulation for dense systems consisting of relevant starlike model macromolecules. In both kinds of systems the two parameters describing the molecular structure of stars, i.e., the arm length and arm number, have been varied in a rather broad range. Unfortunately, because of limited availability of well-defined samples of star polymers with very short arms, on one hand, and limits in sizes of model systems in computer simulations, on the other hand, the ranges of parameters of the two kinds of systems do not overlap. Nevertheless, the results obtained by both types of investigation techniques seem to provide the same qualitative picture concerning both the structure and the dynamics of melts of star molecules and, therefore, supporting each other.

The most important observation concerning structure is related to the ordering of stars in the melt when the number of arms is sufficiently high. Experimentally, it was observed for specific multiarm star macromolecules in which advantage has been taken of the electron density contrast between the dendritic center and the arms. For systems without such specific star centers, no significant scattering other than local segmental fluctuations in the melt can be expected. This is a reason in our investigation no X-ray scattering measurements on 18-arm polyisoprene stars are included; however, according to the simulation results, some limited degree of order could already appear in these systems. The ordering effect of the stars in melts has been characterized more extensively through an analysis of the structure in simulated systems. The analysis of intrastar density distributions (Figure 5), described in more detail in a former publication,[12] has shown that for stars with an arm number exceeding 24 a central core range can be distinguished that is exclusively occupied by segments of the given star and remains impenetrable for arms of neighboring stars. The same effect, which can be considered as an excluded volume effect on the macromolecular scale, has been demonstrated here in Figure 3, in which the pair correlation functions of star centers of mass indicate a wide range of small distances between star centers which is not accessible when the number of arms is sufficiently high. This limitation in center-to-center distances for multiarm stars must result in the observed order. It was not possible to test at which number of arms the real systems start to order. Our polybutadiene samples, for which the ordering was possible to observe, had numbers of arms exceeding the expected limiting value by at least a factor of 2. Any synthetic effort to get more samples with stars having numbers of arms in the necessary range would be useful in this context.

Both the experimental and simulation results have shown that the degree of order in star polymer melts depends on both molecular parameters, the number and the length of arms. It can be supposed that the degree of order in the studied systems is mainly controlled by the ratio of the core radius to corona thickness, which evidently depends on these parameters. Therefore, for stars with a large number of short arms, the highest degree of ordering should be expected, whereas stars with long arms could show a limited order, even when the number of arms is high.

The type of order observed in the multiarm star melts can be described as liquidlike on the macromolecular scale. Neither in real nor in simulated systems have been detected any clear signatures of lattice formation. This results probably from the deformability and related form fluctuations of the star coronas. They consist of flexible arms and remain soft spheres even when f is large and the core radius is large. The latter is well-confirmed by the dynamic properties of the studied systems.

Qualitatively, the simulation results concerning dynamics seem also to be in good agreement with the experimental observations. The suggested assignments of the relaxations detected by means of the viscoelastic measurements appear to be reflected in the simulation. Two relaxations, one related to segmental motion and the other to relaxation of the star arm, are observed in all systems. The relaxation rate of segmental motion is independent of star structure parameters, both in experiments and in the simulation. On the other hand, the relaxation of the star arm has been observed to be considerably dependent on the arm length but essentially independent of the arm number. The most interesting effect observed both in the simulated and in the real systems was the additional slow relaxation process appearing in systems with clear ordering of stars. The analysis of the simulation results concerning dynamics, as well as observation of star motions in these systems (Figure 15), led us to the concept that this slow process can be related to translational cooperative rearrangements of stars within the ordered state. This might be a cooperative process on the macromolecular scale, however, with the mechanism analogous to that postulated recently for liquids.[22]

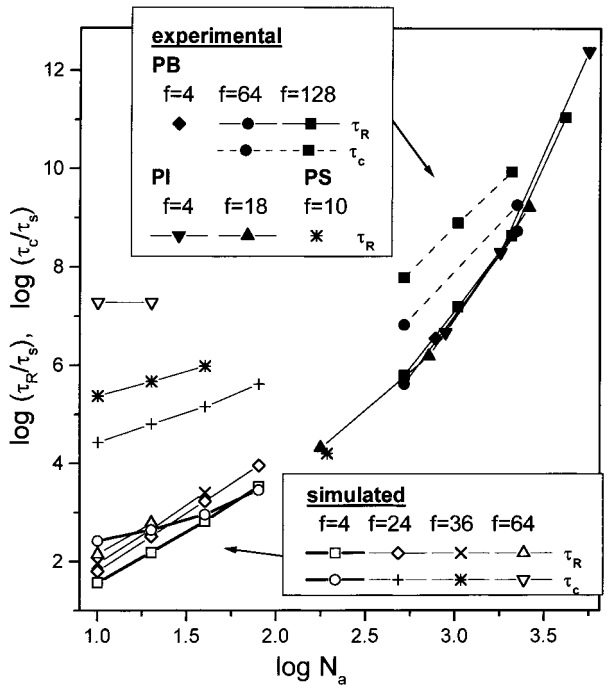

Figure 16. A comparison of arm length dependencies of the reduced relaxation times τ_R/τ_s and τ_c/τ_s for simulated and experimentally studied systems. Lengths of arms in simulated systems are given by the number of beads, whereas the arm length in real systems is expressed by the number of bonds in the arm backbone.

To make a quantitative comparison between the experimental and simulation results, reduced relaxation times (normalized by the segmental relaxation times) of the two slower processes detected by both investigation methods are shown in Figure 16 as a function of arm length and various functionalities. The length of arms (N_a) in simulated systems is given by the number of beads, whereas in the real systems, it is expressed by the number of bonds in the arm backbone. It has been demonstrated earlier for linear polyisoprene chains[14] that this kind of representation of chain lengths leads to a good agreement between the reduced chain relaxation times determined for simulated and real systems. In Figure 16, results for both polyisoprene and polybutadiene stars are considered. Additionally, the polystyrene arm relaxation time for the 10-arm macromonomer (section II) is shown. For all these polymers the τ_R/τ_s times constitute a common dependence. This indicates again that the corresponding relaxation is mainly controlled by the length of star arms and is independent of the arm number, at least for longer arms. Inspite of the gap between the ranges of arm lengths for simulated and real systems, the τ_R dependencies for both kinds of systems seem to extend each other in a similar way, as was earlier observed for melts of linear chains.[14] The reduced relaxation times τ_R/τ_s for both polybutadiene and polyisoprene stars are also presented in a semilog plot (Figure 17), which indicates that the exponential dependence on the arm length suggested by the theory[23] can only be attributed to systems with arm lengths $N_a > 1200$, which corresponds nearly to $M_a > 20\,000$ and $M_a > 16\,000$ for polyisoprene and polybutadiene, respectively. These values are remarkably higher than the entanglement molecular weights for melts of corresponding linear chain polymers.

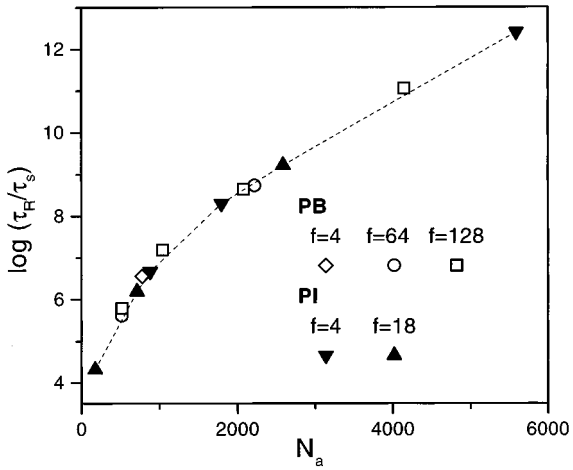

Figure 17. Arm length dependence of the reduced arm relaxation times for polybutadiene and polyisoprene star melts. The dashed line connects the points for polyisoprene.

The agreement between the relaxation times related to the slowest relaxation (τ_c/τ_s) in simulated and real star melts seems to be less satisfactory. A limited number of points in both groups of results and consequently a larger gap between them on the arm length scale do not allow us to make here a final conclusion. Nevertheless, both kinds of results (simulation and experiments) indicate that the slowest process can be observed only for a large number of arms and that the corresponding relaxation times are less dependent on the arm length than the arm relaxation times. Consequently, an increase of the number of arms and a decrease of arm length lead to larger separation between the two slow relaxation processes.

Generally, two kinds of melts of polymer stars can be distinguished as extremes with considerably different structure and dynamic properties. The first kind is melts containing stars with a small number of arms or stars with very long arms which do not order and for which the terminal dynamics is mainly controlled by the arm relaxation. The second kind of melts includes stars with a large number of relatively short arms which show a distinct ordering and in which the slowest dynamics is controlled by structural rearrangements. The first group can rather be considered as a typical polymeric system, but the second group shows analogies to colloids.

V. Conclusions

Melts of multiarm stars have a well-ordered structure similar to that of dense colloidal systems. Central parts of stars with a sufficiently high number of arms can be considered as cores occupying a volume excluded for elements of neighboring stars. Because of this excluded volume effect, the centers of mass of multiarm stars show distinct correlation of positions with respect to neighbors.

This structure involves considerable changes in the dynamics of multiarm star melts with respect to melts composed of stars with a low number of arms. The flow of such systems becomes controlled not by the relaxation of the star arm but by an additional slow relaxation process which is attributed to cooperative rearrangements of stars within the ordered state.

Computer simulations and experimental results provided a very consistent picture concerning both the structure and the dynamics in studied systems.

Acknowledgment. We are grateful to Dr. P. Lutz for generously providing the polystyrene macromonomer used in this work.

References and Notes

(1) Doi, M.; Edwards, S. F. *The theory of polymer dynamics*: Oxford: New York, 1986.
(2) deGennes, P. G. *Scaling concepts in polymer physics*; Cornell University Press: Ithica, NY, 1979.
(3) McLeish, T. C. B. *Phys. World* **1995**, 3, 32. McLeish, T. C. B. In *Chemical Technology: Introduction and Fundamentals;* Bouchev, D., Rouvray, D. H., Eds.; Springer: New York, 1998. McLeish, T. C. B., Ed. *Theoretical Challenges in the Dynamics of Complex Fluids;* NATO ASI, Series E; Kluwer: New York, 1997; Vol. 399.
(4) Hatzikiriakos, S. G.; Kazatchkov, I. B.; Vlassopoulos, D. *J. Rheol*. **1997**, 41, 1299.
(5) Halperin, A.; Tirell, M.; Lodge, T. P. *Adv. Polym. Sci.* **1992**, 31, 100. Vlassopoulos, D.; Pakula, T.; Fytas, G.; Roovers, J.; Karatasos, K.; Hadjichristidis, N. *Europhys. Lett.* **1997**, 39, 617.
(6) Gast, A. P. *Langmuir* **1996**, *12*, 4060.
(7) Russel, W. B.; Saville, D. A.; Schowalter, W. R. *Colloidal dispersions*; Cambridge: New York, 1989.
(8) Roovers, J.; Zhou, L.-L.; Toporowski, P. M.; van der Zwan, M.; Iatron, H.; Hadjichristidis, N. *Macromolecules* **1993**, *25*, 4324.
(9) Grest, G. S.; Fetters, L. J.; Huang, J. S. Richter, D. *Adv. Chem. Phys*. **1996**, *XCIV*, 65. Grest, G.; Kremer, K.; Milner, S. T.; Witten, T. A. *Macromolecules* **1989**, *22*, 1904. Richter, D. *J. Phys.* **1993**, *IV3*, c8, 3.
(10) Seghrouchni, R.; Petekidis, G.; Vlassopoulos, D.; Fytas, G.; Semenov, A. N.; Roovers, J.; Fleischer, G. *Europhys. Lett.* **1998**.
(11) Roovers, J. *J. Non-Cryst.Solids* **1991**, *131−133*, 793.
(12) Pakula, T. *Comput. Theor. Polym. Sci.* **1998**, *8*, 21.
(13) Boese, D.; Kremer, F.; Fetters, L. J. *Macromolecules* **1990**, *23*, 1826.
(14) Pakula, T.; Geyler, S.; Edling, T.; Boese, D. *Rheol. Acta* **1996**, 35, 631.
(15) Ghanou, Y.; Lutz, P. *J. Macromol. Chem*. **1991**, 190, 577. Ederle, Y.; Isel, F.; Grutke, S.; Lutz, P. J. *Macromol. Symp.* 1997.
(16) Ferry, J. D. *Viscoelastic properties of polymers*, 3rd ed.; John Wiley: New York, 1980.
(17) Guinier, A. *X-ray Diffraction*; Freeman & Co.: San Francisco, 1963.
(18) Daoud, M.; Cotton, J. P. *J. Phys. (Paris)* **1982**, *45*, 531. Förster, S.; Wenz, E.; Lindner, P. *Phys. Rev. Lett.* **1996**, 77, 95.
(19) Milner, S. T.; McLeish, T. C. B. *Macromolecules* **1997**, *30*, 2159. Ball, R. C.; McLeish, T. C. B. *Macromolecules* **1989**, *22*, 1911.
(20) Fetters, L. J.; Kiss, A. D.; Pearson, D. S.; Quack, G. F.; Vitus, F. J. *Macromolecules* **1993**, *26*, 647. Adams, C. H.; Hutchings, L. R.; Klein, P. G.; McLeish, T. C. B.; Richards, R. W. *Macromolecules* **1996**, *29*, 5717.
(21) Fleischer, G.; Vlachos, G.; Vlassopoulos, D.; Fytas, G.; Roovers, J. Unpublished data.
(22) Pakula, T.; Teichmann, J. *Mater. Res. Soc. Symp. Proc.* **1997**, *455*, 211.
(23) De Genes, P. G. *J. Phys. (Paris)* **1975**, *36*, 1199.

MA981043R